

# Calculation of Protein Form Birefringence Using the Finite Element Method

Zorica Pantic-Tanner\* and Don Eden<sup>#</sup>

\*School of Engineering and <sup>#</sup>Department of Chemistry and Biochemistry, San Francisco State University, San Francisco, California 94132 USA

**ABSTRACT** An approach based on the finite element method (FEM) is employed to calculate the optical properties of macromolecules, specifically form birefringence. Macromolecules are treated as arbitrarily shaped particles suspended in a solvent of refraction index  $n_1$ . The form birefringence of the solution is calculated as the difference in its refractive index when all the particles of refractive index  $n_2$  are either parallel to or normal to the direction of the polarization of light. Since the particles of interest are small compared to the wavelength of light, a quasi-static approximation for the refractive index is used, i.e., that it is equal to the square root of the dielectric constant of the suspension. The average dielectric constant of the mixture is calculated using the finite element method. This approach has been tested for ellipsoidal particles and a good agreement with theoretical results has been obtained. Also, numerical results for the motor domains of ncd and kinesin, small arbitrarily shaped proteins with known x-ray structures, show reasonable agreement with the experimental data obtained from transient electric birefringence experiments.

## INTRODUCTION

Electrooptic techniques (Fredericq and Houssier, 1973; O’Konski, 1976; Berne and Pecora, 1976; Krause, 1981) have proved to be very useful for the investigation of biological and other macromolecules. Furthermore, measurement of dynamic light scattering and other electrooptic techniques can be used for probing translational, rotational, and intermolecular motions of macromolecules in solutions (Pecora, 1990; Eden and Elias, 1983; Lewis et al., 1986; Antosiewicz and Porschke, 1989). These measurements yield information about structural properties such as the molecular shape and size, and can give an insight into molecular function. To complement these experimental techniques and aid in the interpretation of the measurement results a number of methods for the calculation of optical properties of macromolecules, such as birefringence or the complete set of observables defined by Mueller matrix (Bohren and Huffman, 1983), have been developed. The analysis of a system of arbitrarily oriented macromolecules is usually carried out in two steps. In the first step, the polarizabilities of a single molecule are calculated. They describe the interaction of the molecule with the electric field of the incident light wave and are used to calculate the scattered field (Stratton, 1941; Bottcher, 1973). In the second step the averaging of the scattered field over all possible molecular orientations is done in order to produce the global value of the birefringence or other observables. The easiest approach is to model a macromolecule as a particle with a

simple geometric shape such as a sphere, an ellipsoid of revolution, or a very long cylinder, for which polarizabilities can be found in closed form (Bohren and Huffman, 1983; Van Bladel, 1964). For example, Bragg and Pippard (1953) have used the ellipsoidal model and Wiener (1912) theory for the form birefringence calculation of hemoglobin crystals and obtained good agreement with measured results of Perutz (1953). Similarly, Shi and McClain (1993) have proposed modeling rod-shaped tobacco mosaic virus as a thin long cylinder and have derived a closed-form solution for the scattered field. However, these simple molecular models are not adequate to describe proteins or other molecules of arbitrary shape. For instance, a series of measurements on the flow birefringence of fibrous protein solutions have failed to agree with the ellipsoidal model and an approach that represents a macromolecule by a chain (necklace) of induced dipoles (point polarizabilities) has been introduced by Taylor and co-workers (Taylor and Cramer, 1963; Cassim and Taylor, 1965; Cassim et al., 1968). Oldenbourg and Ruiz (1989) have combined the two approaches to produce a more accurate method for birefringence calculation. They have first divided the macromolecule into subunits of simple geometrical shapes and then have applied Wiener’s theory to obtain the effective dielectric constant, and birefringence, of the overall structure using the known depolarizing coefficients of each subunit. Tian and McClain have additionally improved the molecular model by taking into account the mutual interaction among the molecular subunits (point polarizabilities) (Tian and McClain, 1989a). In one of their papers Tian and McClain (1989b) have used a so-called “pseudo-tetrahedral model,” i.e., four spheres located at the vertices of a tetrahedra, “intended to resemble, in size and total polarizability (but not in shape and symmetry) a particle rather like a picornavirus, responsible for polio, AIDS, and the common cold.” Starting from the polarizabilities of a single sphere

*Received for publication 30 December 1997 and in final form 26 February 1999.*

Address reprint requests to Dr. Zorica Pantic-Tanner, School of Engineering, San Francisco State University, 1600 Holloway Ave., SCI 165, San Francisco, CA 94132. Tel.: 415-338-7739; Fax: 415-338-0525; E-mail: zpt@sfsu.edu.

© 1999 by the Biophysical Society

0006-3495/99/06/2943/08 \$2.00

they have calculated the actual polarizabilities of each sphere due to mutual interactions and then found the total scattered field. A similar approach has been used by Shapiro et al. (1994) to calculate the Mueller matrix for a DNA plactonemic helix.

Since real biological macromolecules are more complicated than these current models, there is a need to develop new models and methods for their analysis. In this paper we use the finite element method (FEM) to calculate the form birefringence. The FEM, originally used in mechanics (Zienkiewicz and Taylor, 1989), has been successfully employed to solve different quasi-static and dynamic electromagnetics problems (Chari and Silvester, 1980; Silvester and Pelosi, 1994; Jin, 1993; Daly, 1984; Manges and Cendes, 1995; Boag and Mittra, 1995; Pantic and Mittra, 1986a,b; 1987). The method is well suited to describe biological problems since they can be reduced to the equivalent electromagnetics problems, e.g., birefringence of the suspension of macromolecules can be calculated from the effective dielectric constant. The advantage of the FEM over the previously mentioned methods is that it is capable of treating real, arbitrarily shaped macromolecules. Moreover, both the macromolecules and the surrounding solvent can be either optically isotropic or anisotropic, as well as homogeneous or inhomogeneous. We have used commercially available FEM software to obtain data necessary for the effective dielectric constant calculation. Numerical results show good agreement with the available measurements.

## QUASI-STATIC FORM BIREFRINGENCE

The birefringence of a suspension of macromolecules is equal to the difference in the refractive index of the suspension for two different orthogonal polarizations of light. For example, if a light wave is propagating along the  $x$  axis of the  $x, y, z$  coordinate system, and its electric field is oriented along the  $y$  axes, the effective refractive index is  $n_y$ . For the  $z$ -polarization of the light wave, i.e., electric field oriented in the  $z$  direction, the effective refractive index is  $n_z$ . The resulting birefringence,  $\Delta n_x$ , is then  $\Delta n_x = n_z - n_y$ . The birefringence may be broken down into two components, the form birefringence and intrinsic birefringence. All non-spherical molecules, even when isotropic and nonpolar, exhibit form birefringence providing that they are partially or fully aligned and the effective index of refraction of the molecule is different from the surrounding solvent. However, intrinsic birefringence arises from the ordered arrangement of intramolecular components with anisotropic optical polarizability, which frequently are due to aromatic rings in biopolymers. The magnitude and sign of the birefringence of a macromolecular system may yield information about its structural properties, such as size and shape, and its orientation in the applied field.

In this paper we are interested in the form birefringence of isotropic homogeneous macromolecules (of refraction index  $n_2$ ) suspended in an isotropic homogeneous solvent

(of refraction index  $n_1$ ). Two assumptions are made about the solution. The first is that the macromolecules, as well as the distances among them, are small compared to the wavelength of light so that a quasi-static approximation for the electric field of the light wave can be used. The second assumption is that the concentration of macromolecules in the suspension is low, which is true in the cases of interest, so that the mutual interactions among molecules are small. Consequently, the form birefringence is calculated as the product of the birefringence for the fully oriented molecules, the saturation form birefringence,  $\Delta n_{\text{sat}}$ , and the orientational order parameter,  $S$ , obtained by averaging the distribution function of the molecules over all angles of orientation (Oldenbourg and Ruiz, 1989). It should be noted that neither of these assumptions is necessary for the FEM application, since the FEM can easily treat macromolecules of arbitrary size and also take into account the mutual interactions among macromolecules.

The saturation form birefringence is usually expressed as  $\Delta n_{\text{sat}} = n_{\parallel} - n_{\perp}$  (Van Bladel, 1964), where  $n_{\parallel}$ ,  $n_{\perp}$  denote the refractive indices of the suspension when the electric field of the incident light wave is parallel to or orthogonal to the optical/electrical axis of the molecular system, respectively. Under the quasi-static approximation for the electric field of the light wave the refractive index is equal to the square root of the effective dielectric constant:  $n_{\parallel} = \sqrt{\epsilon_{\parallel}}$  and  $n_{\perp} = \sqrt{\epsilon_{\perp}}$ . Hence, the optical problem can be reduced to an electromagnetics one of finding the effective dielectric constant (permittivity).

## CALCULATIONAL METHODS

The task of the form birefringence calculation is broken down into the following subtasks: 1) definition of the equivalent electromagnetic field problem; 2) calculation of a macromolecule orientation in the applied external field, i.e., finding its electrical axis; 3) stereolithic modeling of a macromolecule; 4) application of the finite element method; and 5) effective dielectric constant and refractive indices calculation.

### Problem definition

In this paper we use the following approach to calculate the saturation form birefringence. The suspension is represented by a three-dimensional (3-D) regular array of macromolecules of refractive index  $n_2$  in a solvent with refractive index  $n_1$ . A strong external electric field is applied in the  $z'$  direction of the local  $x', y', z'$  coordinate system. Since the molecules are polar, their equivalent dipole moments,  $\mu$ , are oriented along the direction of the external field due to the resulting electric forces. Hence, the system consists of molecules that are fully aligned in the  $z'$  direction as shown in Fig. 1. Now we find the refractive indices of the suspension  $n_{\parallel}$  and  $n_{\perp}$  when the polarization of the incident light wave is parallel and orthogonal, respectively, to the  $z'$  axis. The refractive index  $n_{z'} = \sqrt{\epsilon_{z'}}$ , where  $\epsilon_{z'}$  is the effective dielectric constant of the suspension when the electric field of the incident light wave is  $z'$ -oriented. Since the macromolecules under consideration are generally not symmetric with respect to their electrical axis (dipole moment), we find the average refractive index for the orthogonal polarization of the light wave as  $n_{\perp} = (n_{x'} + n_{y'})/2 = (\sqrt{\epsilon_{x'}} + \sqrt{\epsilon_{y'}})/2$ , where  $\epsilon_{x'}$  and  $\epsilon_{y'}$  are the effective dielectric constants of the suspension when the electric field of the incident light wave is  $x'$ - and  $y'$ -oriented, respectively.

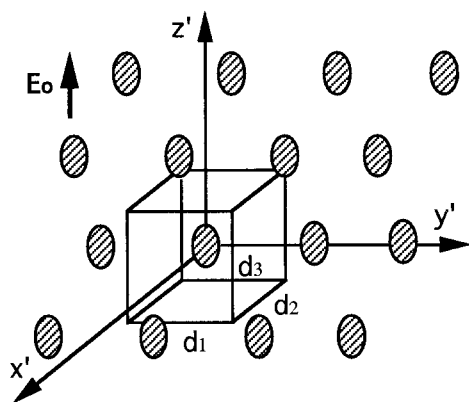


FIGURE 1 Regular 3-D lattice of particles suspended in a solvent, and a unit cell with a single particle.

The problem is now reduced to finding the effective dielectric constants  $\epsilon_{x'}$ ,  $\epsilon_{y'}$ , and  $\epsilon_{z'}$ . For example, to calculate  $\epsilon_{z'}$  we use an incident light wave with  $z'$  polarization and find its interaction with the suspension. The electric field of the light wave is  $z'$ -oriented and is represented by a uniform quasi-electrostatic field,  $E_0$ . Due to the symmetry of the system the periodic 3-D array problem can be reduced to that of a single macromolecule located at the center of a unit bricklike cell (Collin, 1991) as shown in Fig. 1. The lengths of the sides of the unit cell are  $d_1$ ,  $d_2$ , and  $d_3$  in the  $x'$ -,  $y'$ -, and  $z'$  directions, respectively. The volume of the cell is  $V_c = d_1 d_2 d_3$ . If the volume of the macromolecule is  $V_m$ , then we can introduce the volume fraction,  $f$ , as  $f = V_m/V_c$ , which represents the volume concentration of macromolecules in the solvent. Hence, by varying the size of the cell we can vary the concentration, and vice versa; for a given concentration of the solution we can calculate the size of the cell.

In order to take into account the mutual interactions among the aligned macromolecules we apply periodic boundary conditions on the walls of the unit cell. These boundary conditions require the normal component,  $E_n$ , of the total electric field to be equal to zero on the walls of the unit cell that are parallel to the quasi-electrostatic field,  $E_0$ . Instead of directly computing the total electric field distribution,  $E$ , it is customary in the quasi-static approximation to use the electric scalar potential,  $\phi$ , which is related to the total electric field as  $E = -d\phi/dn$ . Accordingly, the incident field  $E_0$ , which is oriented along the  $z'$  axis, can be modeled by setting potentials of the top and bottom faces of the unit cell to  $-E_0 d_3/2$  and  $E_0 d_3/2$ , respectively, where  $d_3$  is the length of the side of the unit cell along the  $z'$  direction (Fig. 2). The periodic boundary condition now requires the

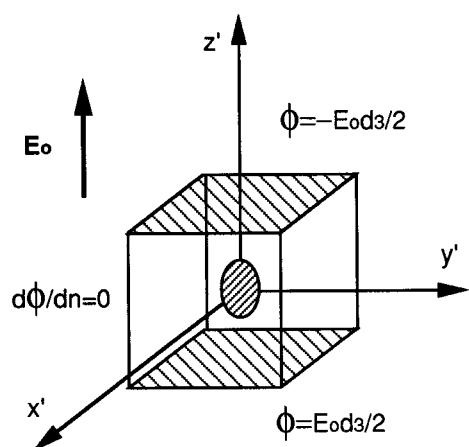


FIGURE 2 Unit cell with a single macromolecule: boundary conditions for  $\epsilon_{z'}$  calculation.

normal derivative of the electric scalar potential  $\phi$  to be equal to zero on the side walls, i.e.,  $E_n = -d\phi/dn = 0$ .

### Macromolecule orientation: electrical axis

Since the protein macromolecules are polar, their orientation in the external electric field is not arbitrary. Rather, they are oriented in such a way that their effective electric dipole moments are aligned with the external field. Hence, the electric axis of the molecule coincides with the direction of its effective electric dipole moment.

The structures of the macromolecules are obtained by using the high-resolution x-ray coordinates of the monomeric units as such as those described by Sablin et al. (1996) and Kull et al. (1996) or by using available PDB files. A commercially available program, Quanta by MSI-BioSym (San Diego, CA), may then be used to calculate the dipole moments from the x-ray structures and therefore the proper orientation of a macromolecule in the applied external electric field.

### Stereolithic modeling of macromolecules

In order to apply the finite element method, a stereolithic model has to be generated, i.e., the shape of the macromolecule and the surrounding solvent has to be described to the computer in an appropriate way. In this study we use the commercially available FEM software package Maxwell by Ansoft Corporation (Pittsburgh, PA) as the best suited for the problems at hand. This package contains a fairly good and flexible solid-modeler. Fig. 3 shows an ellipsoidal model of a molecule generated by this program. The Maxwell modeler can also generate a sphere, cylinder, cube, or a similar model, or any other body that consists of these basic shapes.

A systematic approach for building more realistic stereolithic models of macromolecules is proposed. Using the structural information, a macromolecule at hand is divided into monomeric units based on high-resolution coordinates obtained by x-ray or electron diffraction. Each unit is represented by a sphere or cube centered at a high-resolution coordinate. The size of the unit is chosen to give an overall volume equal to that of the hydrated macromolecule in solution. These simple models provide for geometrical repetitiveness and uniformity. The cube is advantageous over the sphere since it results in a smaller number of finite elements and thus requires less memory and CPU time. A stereolithic model is built in the following way. First, a generic monomeric unit (building block), centered at the coordinate origin, is generated. Second, it is copied to the appropriate positions defined by the high-resolution coordinates. Third, all individual

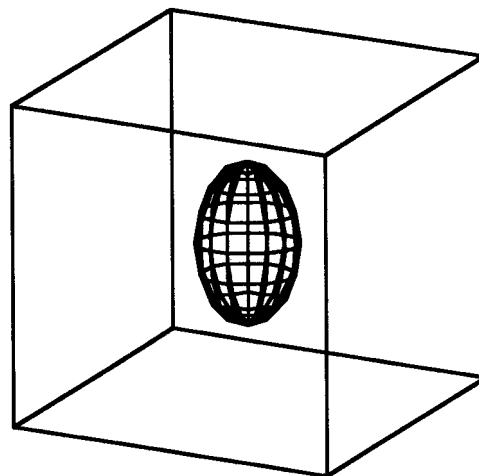


FIGURE 3 Stereolithic model of an ellipsoidal molecule, and surrounding solvent with semiaxes  $a = b = 2.32 \text{ \AA}$ ,  $c = 5.00 \text{ \AA}$ ,  $d_1 = d_2 = d_3 = d = 10 \text{ \AA}$ ,  $f = 10.3\%$ .

units generated in this manner are united to produce a solid object that represents the overall model of the molecule. The molecule is then placed in the center of a prismlike unit cell that represents the surrounding solvent. As explained previously, the size of the cell depends on the concentration of the solution. The orientation of the molecule is such that its electrical axis, as calculated by Quanta, is oriented along the  $z'$  axis. Fig. 4 shows a stereolithic model of *Drosophila* ncd(335-700), a molecular motor, built with cubic monomeric units with edges of 9 Å that are centered at the coordinates of  $\alpha$ -carbons of this protein (Sablin et al., 1996). The volume of the model is 70,700 Å<sup>3</sup>, which is consistent with the known molecular weight, a specific volume of 0.73 cm<sup>3</sup>/g, and hydration of 0.30 g<sub>water</sub>/g<sub>ncd</sub>.

## The finite element method

The 3-D electrostatic field program that is part of the Maxwell package (Ansoft Co., Pittsburgh, PA), and that employs the finite element method is used to find the potential distribution and electric energy within the unit cell (Chou and Cendes, 1994).

The general idea of the finite element method is quite simple and straightforward. The global configuration of the cell containing a macromolecule is divided into a number of small 3-D elements with regular geometric shapes of different sizes, such as tetrahedra. The physical/optical properties of each element can be different from those of the others but are constant within each element. Within each element several nodal points are defined. The electric scalar potential,  $\phi_e$ , within each element is approximately represented by the values of the potential at the nodal points,  $\Phi_i$ , and appropriate interpolation functions,  $\alpha_i$ ,

$$\phi_e = \sum_{i=1}^M \Phi_i \alpha_i(x, y, z) \quad (1)$$

where  $M$  is the number of nodes per element. If a linear approximation of the potential function is used, the element has four nodes located at the vertices of the tetrahedron, as shown in Fig. 5. A quadratic element has 10 nodes; an additional six nodes are placed at the middle of the tetrahedron edges (Fig. 5). The Maxwell 3-D static solver uses second-order elements (Cendes et al., 1981).

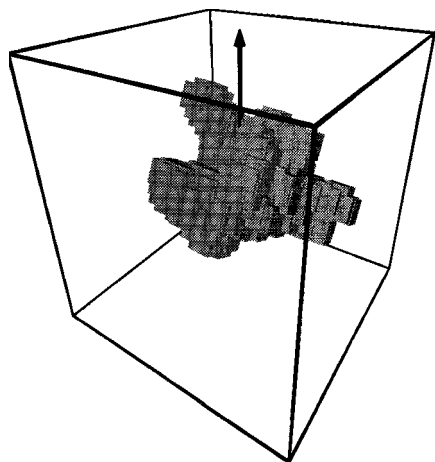


FIGURE 4 Stereolithic model of a *Drosophila* ncd(335-700) based on the union of cubes having 9-Å sides, and yielding molecular volume of 70,700 Å<sup>3</sup>. The arrow represents the direction of the electric dipole moment and the  $z'$  axis used in the calculations.

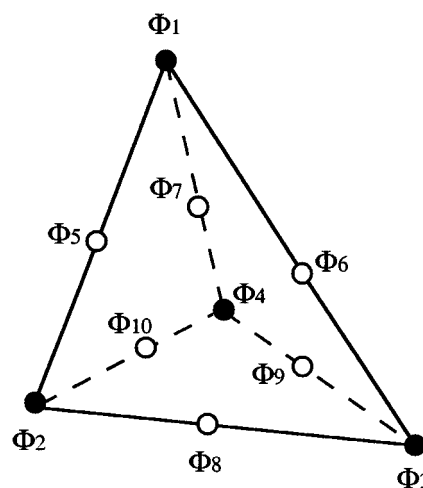


FIGURE 5 Quadratic element with 10 nodes.

The global electric energy,  $W$ , of the cell is expressed in terms of these nodal values

$$\begin{aligned} W &= \sum_{e=1}^N \frac{1}{2} \epsilon_e \int_{v_e} |\nabla \phi_e|^2 dv_e \\ &= \sum_{e=1}^N \frac{1}{2} \epsilon_e \int_{v_e} \sum_{i=1}^M \sum_{j=1}^M \Phi_i \Phi_j \nabla \alpha_i \nabla \alpha_j \end{aligned} \quad (2)$$

where  $N$  is the total number of elements,  $v_e$  is the volume of the  $e$ th element, and  $\epsilon_e$  is the dielectric constant of the  $e$ th element. A variational principle that minimizes this energy is used to produce a system of linear algebraic equations involving only the nodal unknowns  $\Phi_i$ ,  $i = 1, 2, \dots, M_t$ , where  $M_t$  is the total number of the nodes in the mesh.

$$\frac{\partial W}{\partial \Phi_i} = \sum_{e=1}^N \epsilon_e \int_{v_e} \sum_{j=1}^M \sum_{k=1}^M \Phi_j \nabla \alpha_i \nabla \alpha_k = 0, \quad i = 1, \dots, M_t \quad (3)$$

The nodal potentials also have to satisfy the appropriate boundary conditions. For example, if  $\epsilon_{z'}$  is to be calculated, the potentials of the nodes on the top and the bottom of the unit cell are equal to  $-E_0 d_3/2$  and  $E_0 d_3/2$ , respectively (Fig. 2), as explained previously. The resulting system of equations is sparse and special solution techniques that take advantage of this property are used (George and Liu, 1981). Once the nodal potentials are known the corresponding energy,  $W_{z'}$ , can easily be found using Eq. 2.

The numerical solution derived from the FEM converges to the exact solution without limit on accuracy as long as the number of elements increases to a sufficiently large value. Actually, in order to increase the accuracy of the solution, the 3-D solver uses an iterative approach with adaptive mesh refinement, i.e., the tetrahedral mesh is refined (divided into smaller elements) where the field changes more rapidly.

## Effective dielectric constants and form saturation birefringence

As explained previously, to find the form birefringence of the macromolecule suspension we need to calculate all three effective dielectric constants,  $\epsilon_{x'}$ ,  $\epsilon_{y'}$ , and  $\epsilon_{z'}$ . For that purpose we apply the finite element method to solve for the energies  $W_{x'}$ ,  $W_{y'}$ ,  $W_{z'}$  in the unit cell resulting from the  $x'$ -,  $y'$ -, and  $z'$ -polarization of the incident electric field  $E_0$ , respectively. Once the distribution of the electric scalar potential in the unit cell, as well as the



total electric energy in the cell, have been found using the finite element method, the corresponding effective dielectric constant can be readily obtained. For example, the effective dielectric constant of the suspension  $\epsilon_{z'}$  can be calculated as  $\epsilon_{z'} = W_{z'}/W_0$ , where  $W_0$  is the energy within the unit cell filled with air (vacuum). The energy  $W_0$  can be found simply as  $W = \epsilon_0 E_0^2 V_c / 2$ , where  $V_c = d_1 d_2 d_3$  is the volume of the unit cell, and  $\epsilon_0 = 8.85 \times 10^{-12}$  F/m is the free space permittivity. Similar procedures are repeated to find  $\epsilon_{x'}$  and  $\epsilon_{y'}$ . Finally, the saturation form birefringence is calculated as  $\Delta n_{\text{sat}} = \sqrt{\epsilon_{z'}} - (\sqrt{\epsilon_{x'}} + \sqrt{\epsilon_{y'}})/2$ .

## NUMERICAL AND EXPERIMENTAL RESULTS

In order to test the accuracy of the proposed FEM approach, the saturation form birefringence of an ellipsoidal molecule with semiaxes  $a$ ,  $b$ ,  $c$ , oriented along  $x'$ ,  $y'$ , and  $z'$  axes, respectively (Fig. 3), was calculated. The molecule was symmetric with respect to the  $z'$  axis, i.e.,  $a = b$ . Also, the geometric axis was considered to be the electric axis. The molecule was placed in a unit cubic cell of sides  $d_1 = d_2 = d_3 = d = 20$  Å. The value of the refractive index of the this molecule was chosen to be equal to that expected for a protein (Bragg and Pippard, 1953),  $n_2 = 1.60$ . The solvent was water with refractive index  $n_1 = 1.33$ . The convergence of the numerical solution for the energy of the unit cell is shown in Table 1. It is apparent that the error in the solution can be reduced to a desired value by using an iterative approach that increases the number of finite elements in the mesh. The FEM results for the saturation form birefringence were compared with the values obtained by using the analytical solutions for dielectric constants  $\epsilon_{x'}$ ,  $\epsilon_{y'}$ , and  $\epsilon_{z'}$  (Wiener, 1912):

$$\epsilon_{x',y',z'} = \epsilon_1 + \frac{f(\epsilon_2 - \epsilon_1)}{1 + (1-f)L_{x',y',z'}(\epsilon_2 - \epsilon_1)/\epsilon_1} \quad (4)$$

In this formula  $f$  is the volume fraction,  $\epsilon_1 = n_1^2$ ,  $\epsilon_2 = n_2^2$  are dielectric constants of the solvent and the macromolecule, respectively, and  $L_{x'}$ ,  $L_{y'}$ , and  $L_{z'}$  are depolarizing coefficients given by Bohren and Huffman (1983) and Stratton (1941):

for prolate spheroid ( $a = b$ ,  $c > a$ )

$$L_{z'} = \frac{1 - e^2}{e^2} \left( -1 + \frac{1}{2e} \ln \frac{1 + e}{1 - e} \right), \quad e^2 = 1 - \frac{a^2}{c^2} \quad (5)$$

$$L_{x'} = L_{y'} = (1 - L_{z'})/2$$

**TABLE 1** Convergence of the electrostatic energy as a function of the number of finite elements in the mesh

Iteration	No. of Tetrahedra	Total Energy	Error (%)
1	640	1.584913	0.0088
2	804	1.584852	0.0077
3	1039	1.584780	0.0043
4	1371	1.584740	0.0019
5	1822	1.584724	0.0012
6	2783	1.584716	0.0008

The quasi-electrostatic field is oriented along the  $z'$ -axis of the cubic unit cell containing an ellipsoid of revolution ( $a = b = 2.32$  Å,  $c = 5.00$  Å,  $d = 20$  Å,  $n_1 = 1.33$ ,  $n_2 = 1.60$ ).

for oblate spheroid ( $a = b$ ,  $c < a$ )

$$L_{z'} = \frac{g(e)}{2e^2} \left( \frac{\pi}{2} - \tan^{-1} g(e) \right), \quad g(e) = \left( \frac{1 - e^2}{e^2} \right)^{1/2}$$

$$e^2 = 1 - \frac{c^2}{a^2} \quad (6)$$

$$L_{x'} = L_{y'} = (1 - L_{z'})/2$$

The relative saturation form birefringence with respect to the refractive index of the solvent,  $\Delta n_{\text{sat}}/n_1$ , is plotted versus the semiaxes ratio  $c/a$  ( $a = b$ ) in Fig. 6. The volume fraction  $f$  is kept constant and fairly low so that the mutual interactions among the neighboring particles are negligible. Very good agreement between the theoretical expressions and numerical results is observed for this dilute sample. For very diluted samples, in order to avoid the round-off errors in the numerical procedures, we used the following approach. We employed the FEM procedure to calculate polarizability coefficients for  $f = 0.0100$ , and then re-scaled the results to the much smaller actual concentration by using Eq. 4.

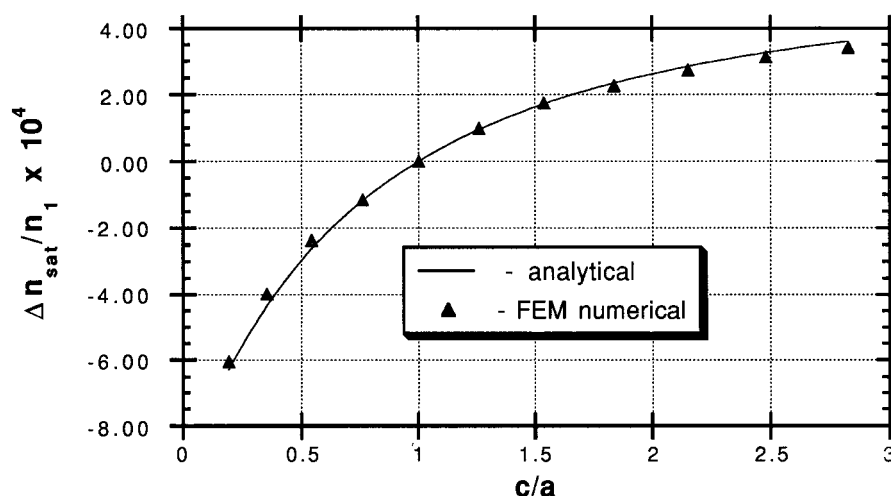
The proposed FEM approach has been applied to several proteins (Pantic-Tanner and Eden, 1996; Pantic-Tanner et al., 1996; Eden et al., 1996). In this paper we present the results obtained for the form birefringence of the motor domain fragments of two molecular motors, kinesin and ncd. We have studied these two molecular motor fragments, which translocate in opposite directions on microtubules. The two 40-kDa proteins have a very similar sequence and x-ray structure (Sablin et al., 1996). The transient electric birefringence (TEB) experiments of Eden et al. (1995) indicate a similar hydrodynamic size as well. However, the sign of the birefringence is opposite in the two motors, suggesting that the effective dipole moments are oriented very differently. This may be important in understanding the different direction of travel. Since the high-resolution coordinates of the ncd and kinesin motors are available (Sablin et al., 1996; Kull et al., 1996), the corresponding stereolithic models have been generated and the form birefringence calculated.

Eden et al. (1995) measured the electric field strength dependence of the steady-state birefringence to obtain specific Kerr constants,  $K_{\text{sp}}$ . In the low electric field limit, the steady-state birefringence is a quadratic function of the field,  $E_0$ , and  $\Delta n = f n K_{\text{sp}}$ , where  $f$  is the volume fraction of the protein and  $n$  the solution index of refraction. Values of  $-1.65 \times 10^{-12} \text{ cm}^2 V^{-2}$  and  $0.36 \times 10^{-12} \text{ cm}^2 V^{-2}$  were determined for ncd(335-700) · Mg · ADP and kinesin(349) · Mg · ADP, respectively in PIPES/NaCl buffer at 4°C. Since the orientation was via a permanent electric dipole moment mechanism, the field strength dependence of the birefringence is given by

$$\Delta n = \Delta n_{\text{sat}} \{1 - (3(\coth \beta - 1/\beta))/\beta\} \quad (7)$$

where  $\beta = \mu E_0 / kT$  is the ratio of the interaction of the effective dipole moment in the applied electric field to the

FIGURE 6 Form birefringence  $\Delta n_{\text{sat}}/n_1$  of ellipsoids versus semiaxis ratio  $c/a$  for a fixed volume fraction  $f$  ( $a = b$ ,  $n_1 = n_{\text{solvent}} = 1.33$ ,  $n_2 = n_{\text{particle}} = 1.60$ ,  $f = 1.32\%$ )



thermal energy. Using the coordinates of the structures for ncd(335-700) · Mg · ADP and kinesin(349) · Mg · ADP, the electric dipole moments calculated by the program Quanta are 975D and 1217D, respectively. [The base of the 975D dipole of ncd(335-700) is at the  $\alpha$ -carbon of ALA 432 and it passes through the carbonyl carbon of ARG 601. The base of the 1217D dipole of kinesin(349) is at the  $\alpha$ -carbon of VAL 230 and it passes through the  $\alpha$ -carbon of THR 315.] The unique value of  $\Delta n_{\text{sat}}$  that satisfies the experimental value of the specific Kerr constant and the calculated dipole moments are  $-3.57 \times 10^{-3}$  and  $5.22 \times 10^{-4}$  for the ncd and kinesin motor domains, respectively.

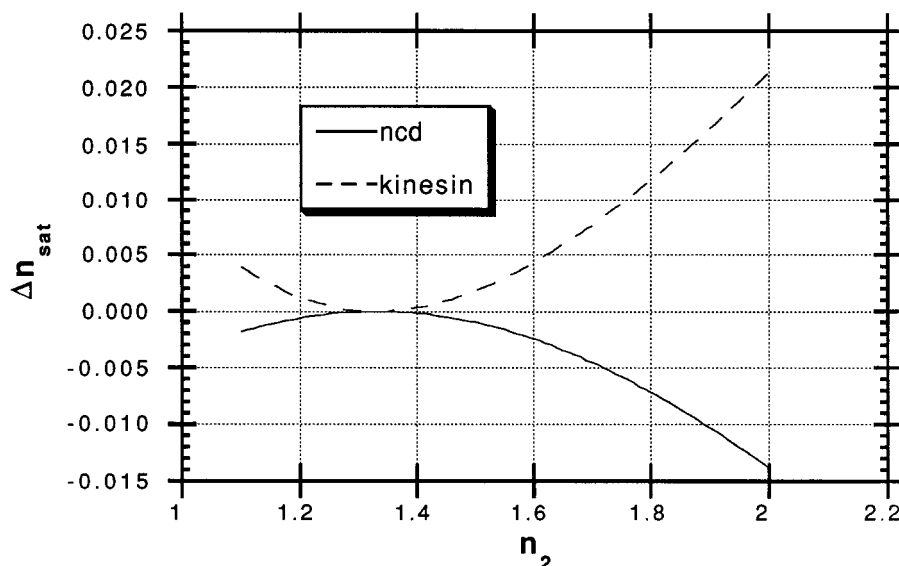
For the ncd motor domain, the FEM calculation yielded  $\Delta n_{\text{sat}} = -2.42 \times 10^{-3}$  using refractive indices of water,  $n_1 = 1.330$ , and that expected for a protein,  $n_2 = 1.600$ , and assuming that the orientation of the molecule was governed by its equivalent dipole moment. By varying the refractive index of the protein, the agreement of the two results was achieved for  $n_2 = 1.665$ , as shown in Fig. 7. The volume concentration of the ncd sample was 0.10%. For the kinesin

molecule, the sign of the FEM result agreed with the TEB experiment but the value of  $4.5 \times 10^{-3}$  was much larger than the measured value. There are two possible causes of the discrepancy between the numerical and experimental results. First, the absence of coordinates for loop L11 in the molecular model might result in an incorrect electric dipole orientation as discussed below. Second, the TEB measurements of the Kerr constant may be inaccurate, as explained previously (Eden et al., 1995).

## DISCUSSION

The agreement between the FEM and analytical calculations of the form birefringence of ellipsoids of revolution, as shown in Fig. 6, demonstrates the power of using the FEM approach to calculate the optical and dielectric properties of macromolecules. However, the application to predicting the electrooptic properties of arbitrary shaped macromolecules requires additional information on the effective dipole mo-

FIGURE 7 Form birefringence  $\Delta n_{\text{sat}}$  of protein solution versus protein refractive index  $n_2$  ( $n_1 = n_{\text{solvent}} = 1.33$ ,  $f = 0.10\%$ , corresponding to the experimental concentration in Eden et al., 1995).



ment of the molecule investigated. The program Quanta assumes point charges with a dielectric constant of one. It ignores the effects of solvent and counterion binding. Although the calculated values of the dipole moments may not quantitatively reflect the electrical properties in the buffered solutions, their relative magnitudes and directions should be reasonable, given the similarity of the structures as determined by x-ray diffraction (Sablin et al., 1996; Kull et al., 1996). As reported previously (Eden et al., 1996), the dipole of the motor domains of the two proteins, which have very similar structures, point in different directions, separated by  $42^\circ$  when the structures are superimposed. This is the principal reason that the values of  $\Delta n_{\text{sat}}$  obtained using the FEM calculations have different signs.

There are additional concerns regarding the available structural data. The crystal structures for ncd(335-700) and kinesin(349) are missing coordinates for  $\sim 12\%$  of the amino acid residues, on the N- and C-termini. Therefore, the calculations of the form birefringence and the dipole moment have additional uncertainties. However, they are not expected to change significantly the quantitative calculations presented above.

Although there is good quantitative agreement between the experimentally predicted and FEM calculated values of  $\Delta n_{\text{sat}}$  for the ncd motor domain, the quantitative agreement for the kinesin motor domain is poor. It is suspected that this discrepancy stems from the fact that the coordinates of loop L11 are not available for the kinesin motor (Kull et al., 1996). In addition, as was discussed previously (Eden et al., 1995), the TEB results of kinesin suggest the formation of nonspecific aggregates that could give rise to either a reduced shape anisotropy or a smaller effective dipole moment. Either could result in a smaller value of the Kerr constant and of  $\Delta n_{\text{sat}}$  than would be expected for the monomeric protein.

## CONCLUSIONS

We have demonstrated that an important optical property, the form birefringence, of an arbitrarily shaped molecule may be calculated using the FEM approach. The advantage of the FEM over the existing numerical methods for birefringence calculation is that it is capable of treating real, arbitrarily shaped macromolecules. Moreover, both the macromolecules and the surrounding solvent can be optically either isotropic or anisotropic, as well as homogeneous or inhomogeneous. This approach provides an opportunity to use the quantitative measurement of birefringence as a tool in determining the structure of biologically important macromolecules. Extension of this approach to solving the full scattering tensor will permit numerous applications in phase microscopy of biological systems.

We gratefully acknowledge R. Oldenbourg for his suggestion to use FEM for the calculation of the form birefringence of arbitrarily shaped particles. A. Der, W. Carrera, B. Q. Luu, M. Bowman, and D. Tomasevich assisted

in the calculations. We thank Daniel Tanner for his assistance with digital artwork.

This work was supported in part by U.S. Public Health Service Grants AM42751 and MBRS SO6 GM52588 (to D.E.) and by a San Francisco State University Faculty assigned time grant (to Z.P.-T.).

## REFERENCES

- Antosiewicz, J., and D. Porschke. 1989. An unusual electrooptical effect observed for DNA fragments and its apparent relation to a permanent electric moment associated with bent DNA. *Biophys. Chem.* 33:19–30.
- Berne, B. J., and R. Pecora. 1976. *Dynamic Light Scattering*. John Wiley, New York.
- Boag, A., and R. Mittra. 1995. A numerical absorbing boundary condition for finite difference and finite element analysis of open periodic structures. *IEEE Trans. Microwave Theory Tech.* 43:150–154.
- Bohren, C. A., and D. R. Huffman. 1983. *Absorption and Scattering of Light by Small Particles*. John Wiley, New York.
- Bottcher, C. J. F. 1973. *Theory of Electric Polarization*, 2nd ed., Vol. 1. Elsevier North-Holland Biomedical Press, Amsterdam.
- Bragg, W. L., and A. B. Pippard. 1953. The form birefringence of macromolecules. *Acta Crystallogr.* 6:865–867.
- Cassim, J. Y., and E. W. Taylor. 1965. Intrinsic birefringence of poly-g-benzyl-L-glutamate, a helical polypeptide, and the theory of birefringence. *Biophys. J.* 5:531–552.
- Cassim, J. Y., P. S. Tobias, and E. W. Taylor. 1968. Birefringence of muscle proteins and the problem of structural birefringence. *Biochem. Biophys. Acta.* 168:463–471.
- Cendes, Z. J., F. U. Minhas, and P. P. Silvester. 1981. Tetrahedral finite element matrix primitives. *Comput. Phys. Commun.* 15:1981.
- Chari, M. V. K., and P. P. Silvester. 1980. *Finite Elements in Electrical and Magnetic Field Problems*. Wiley, Chichester, England.
- Chou, T. Y., and Z. J. Cendes. 1994. Capacitance calculation of IC packages using the finite element method and planes of symmetry. *IEEE Trans. Comp. Aided Design of IC.* 13:1159.
- Collin, R. E. 1991. *Field Theory of Guided Waves*. IEEE Press, Piscataway, New Jersey.
- Daly, P. 1984. Upper and lower bounds to the characteristic impedance of transmission lines using the finite-element method. *Int. J. Comp. Math. Elect. and Elect. Eng.* 3:65–78.
- Eden, D., and J. G. Elias. 1983. Transient electric birefringence of DNA restriction fragments and the filamentous virus Pf3. In *Measurement of Suspended Particles by Quasi-Elastic Light Scattering*. B. E. Dahneke, editor. Wiley, New York. 401–438.
- Eden, D., B. Luu, and Z. Pantic-Tanner. 1996. Molecular motors: power stroke and dipole orientation of kinesin and ncd determined by transient electric birefringence. *Prog. Biophys. Mol. Biol.* 65:173S. (Abstr.)
- Eden, D., B. Q. Luu, D. J. Zapata, E. P. Sablin, and F. J. Kull. 1995. Solution structure of two molecular motors: nonclaret disjunctional and kinesin. *Biophys. J.* 68:59s–65s.
- Fredericq, E., and C. Houssier. 1973. *Electric Dichroism and Electric Birefringence*. Clarendon Press, Oxford.
- George, A., and J. Liu. 1981. *Computer Solution of Large Sparse Positive Definite Systems*. Prentice Hall, Englewood Cliffs, New Jersey.
- Jin, J. M. 1993. *The Finite Element Method in Electromagnetics*. John Wiley, New York.
- Krause, S. 1981. *Molecular Electrooptics: Electrooptic Properties of Macromolecules and Colloids in Solutions*. Plenum Press, New York.
- Kull, J. F., E. Sablin, R. Lau, R. Fletterick, and R. D. Vale. 1996. Crystal structure of the kinesin motor domain reveals a structural similarity to myosin. *Nature.* 380:550–555.
- Lewis, R. J., R. Pecora, and D. Eden. 1986. Transient electric birefringence measurements of the rotational and internal bending modes in monodisperse DNA fragments. *Macromolecules.* 19:134–139.
- Manges, J., and Z. Cendes. 1995. A generalized tree-cotree gauge for magnetic field computation. *IEEE Trans. Magn.* 31:1342–1347.
- O'Konski, C. T. 1976. *Molecular Electrooptics*. Dekker, New York.

- Oldenbourg, R., and T. Ruiz. 1989. Birefringence of macromolecules. *Biophys. J.* 56:195–205.
- Pantic, Z., and R. Mittra. 1986a. Quasi-TEM analysis of isolated and coupled microwave transmission lines. *IEEE Trans. Microwave Theory Tech.* 34:1096–1103.
- Pantic, Z., and R. Mittra. 1986b. Quasi-TEM analysis of isolated and coupled microwave transmission lines by the finite element method. *DAAG 29-85-K-0183*, EMC Report, No. 86-2, University of Illinois, Urbana-Champaign.
- Pantic, Z., and R. Mittra. 1987. Full-wave analysis of isolated and coupled microwave transmission lines. *DAAG 29-85-K-0183*, EMC Report, No. 87-1, University of Illinois, Urbana-Champaign.
- Pantic-Tanner, Z., and D. Eden. 1996. Form birefringence calculations using the finite element method. *Biophys. J.* 70:181a. (Abstr.)
- Pantic-Tanner, Z., S. Pantic, and D. Eden. 1996. Birefringence calculation using the finite element method. *Proc. Antennas and Propagation and Radio Science Symp.* Baltimore:126 (Abstr.)
- Pecora, R. 1990. Dynamic light scattering from macromolecules. In *Selected papers on Quasielastic Light Scattering by Macromolecular, Supramolecular, and Fluid Systems*. USA:SPIE, Optical Engineering Press, Bellingham, WA. 2–15.
- Perutz, M. F. 1953. Polarization dichroism, form birefringence and molecular orientation in crystalline haemoglobins. *Acta Crystallogr.* 6:859–864.
- Sablin, E., J. F. Kull, R. Cooke, R. D. Vale, and R. J. Fletterick. 1996. Crystal Structure of the motor domain of the kinesin-related motor ncd. *Nature*. 380:555–559.
- Shapiro, D. B., A. J. Hunt, and J. E. Hearst. 1994. Calculations of the Mueller scattering matrix for a DNA placentomic helix. *J. Chem. Phys.* 101:4214–4225.
- Shi, Y., and W. M. McClain. 1993. Closed-form Mueller scattering matrix for a random ensemble of long, thin cylinders. *J. Chem. Phys.* 98:1695–1711.
- Silvester, P., and G. Pelosi. 1994. *Finite Elements for Wave Electromagnetics: Methods and Techniques*. IEEE Press, Piscataway, New Jersey.
- Stratton, J. A. 1941. *Electromagnetic Theory*. McGraw-Hill, New York.
- Taylor, E. W., and W. Cramer. 1963. Birefringence of protein solutions and biological systems, I and II. *Biophys. J.* 3:127–154.
- Tian, D., and W. M. McClain. 1989a. Nondipole scattering by partially oriented ensembles. I. Numerical calculations and symmetries. *J. Chem. Phys.* 90:4783–4794.
- Tian, D., and W. M. McClain. 1989b. Nondipole scattering by partially oriented ensembles. III. The Mueller pattern for achiral macromolecules. *J. Chem. Phys.* 91:4435–4439.
- Van Bladel, J. 1964. *Electromagnetic Fields*. McGraw-Hill, New York.
- Wiener, O. 1912. Die Theorie des mischkorpers fur das feld der stationaren stromung erste abhandlung. Die mittelwerstaze fur kraft, polarisation und energie. *Abhandl. Math. Klas. Kongl. sachs. Gesellsch. Wissensch.* 23:509–604.
- Zienkiewicz, O. C., and R. L. Taylor. 1989. *The Finite Element Method in Structural and Continuum Mechanics*. McGraw-Hill, New York.